

BASIC SCIENCE ARTICLE



KIF5C deficiency causes abnormal cortical neuronal migration, dendritic branching, and spine morphology in mice

Wanxing Li¹, Tianling Cheng², Xinran Dong³, Huiyao Chen³, Lin Yang⁴, Zilong Qiu⁵ and Wenhao Zhou^{1,4,6}✉

© The Author(s), under exclusive licence to the International Pediatric Research Foundation, Inc 2021

BACKGROUND: Malformation of cortical development (MCD) includes a variety of developmental disorders that are common causes of neurodevelopmental delay and epilepsy. Most recently, clinical studies found that patients carrying *KIF5C* mutations present early-onset MCD; however, the underlying mechanisms remain elusive.

METHODS: *KIF5C* expression level was examined in mouse primary cortical neurons and human ips-derived forebrain organoids. We studied the cortical neuronal migration, dendritic branching, and dendritic spine growth after knocking down the *KIF5C* gene by electroporation in vitro and in vivo. Then, we studied the transcriptome differences between the knockdown and control groups through RNA sequencing.

RESULTS: We observed high *KIF5C* expression in neurons during the early developmental stage in mice and the human brain. *Kif5c* deficiency results in disturbed cortical neuronal migration, dendritic, and spine growth. Finally, we found that *Kif5c* knockdown affected several genes associated with cortical neuronal development in vitro.

CONCLUSIONS: These results suggested a critical role for *Kif5c* in cortical development, providing insights into underlying pathogenic factors of kinesins in MCD.

Pediatric Research (2022) 92:995–1002; <https://doi.org/10.1038/s41390-021-01922-8>

IMPACT:

- *KIF5C* mutation-related MCD might be caused by abnormal early cortical neuronal development.
- *Kif5c* deficiency led to abnormal cortical neuronal dendritic and spine growth and neuronal migration.
- Our findings explain how *Kif5c* deficiency is involved in the aberrant development of cortical neurons and provide a new perspective for the pathology of MCD.

INTRODUCTION

Precisely controlled dendritic arborization, spine morphogenesis, and neuronal migration ensure functional neural circuit assembly and neural network integrity during cortical development.¹ Abnormal neurite patterning and disturbed neuronal positioning result in various MCD, including lissencephaly/pachygyria (LIS), polymicrogyria (PMG), and microcephaly.^{2–5} These disorders have been observed in individuals with neurodevelopmental disorders, such as seizures, intellectual disability, Rett syndrome, and autism spectrum disorder (ASD).^{6–9} Therefore, it is necessary to find the factors that regulate the growth and migration of neurons in the early stage of cortical development to understand the possible molecular mechanisms of the pathogenesis of MCD.

The *KIF5C* gene encodes heavy chain isoform 5C of kinesin, a microtubule-dependent motor protein that generates force during intraneuronal transport. It transports various cargos, including

vesicles, membranous organelles, protein complexes, mRNAs, and chromosomes, over long distances along neuronal microtubules. These molecular motors are expected to play critical roles in several processes in the brain, including neuronal function, development, survival, and plasticity, by regulating transport within the axons, dendrites, and synapses of neurons.^{10–13}

Previous studies have provided evidence that kinesin superfamily members play a fundamental role in early brain development. In vivo knockout of the *Kif1a*, *Kif1b*, *Kif2a*, *Kif3a*, *Kif3b*, *Kif4a*, *Kif5a*, *Kif5b*, or *Kif5c* genes result in various neurological phenotypes, including brain structural malformation, abnormal brain size, disturbed neuronal proliferation or apoptosis, altered synapse density, and even perinatal death due to severe neurological problems.^{13–23} The early embryonic death of *Kif1b*, *kif2a*, *Kif3a/3b*, and *Kif5b* knockout mice suggests an essential function in general developmental processes as well.^{16–18,23}

¹Division of Neonatology, Children's Hospital of Fudan University, 201102 Shanghai, People's Republic of China. ²Institute of Pediatrics, Children's Hospital, Institutes for Translational Brain Research, State Key Laboratory of Medical Neurobiology, MOE Frontiers Center for Brain Science, Fudan University, 200032 Shanghai, People's Republic of China. ³Center for Molecular Medicine of Children's Hospital of Fudan University, 201102 Shanghai, People's Republic of China. ⁴Key Laboratory of Birth Defects, Children's Hospital of Fudan University, 201102 Shanghai, People's Republic of China. ⁵Institute of Neuroscience, State Key Laboratory of Neuroscience, CAS Center for Excellence in Brain Science and Intelligence Technology, Shanghai Center for Brain Science and Brain-Inspired Intelligence Technology, Chinese Academy of Sciences, 200032 Shanghai, People's Republic of China. ⁶Key Laboratory of Neonatal Diseases, Ministry of Health, Children's Hospital of Fudan University, 201102 Shanghai, People's Republic of China.

✉email: zhouwenhao@fudan.edu.cn

Received: 26 August 2021 Revised: 18 November 2021 Accepted: 13 December 2021

Published online: 29 December 2021

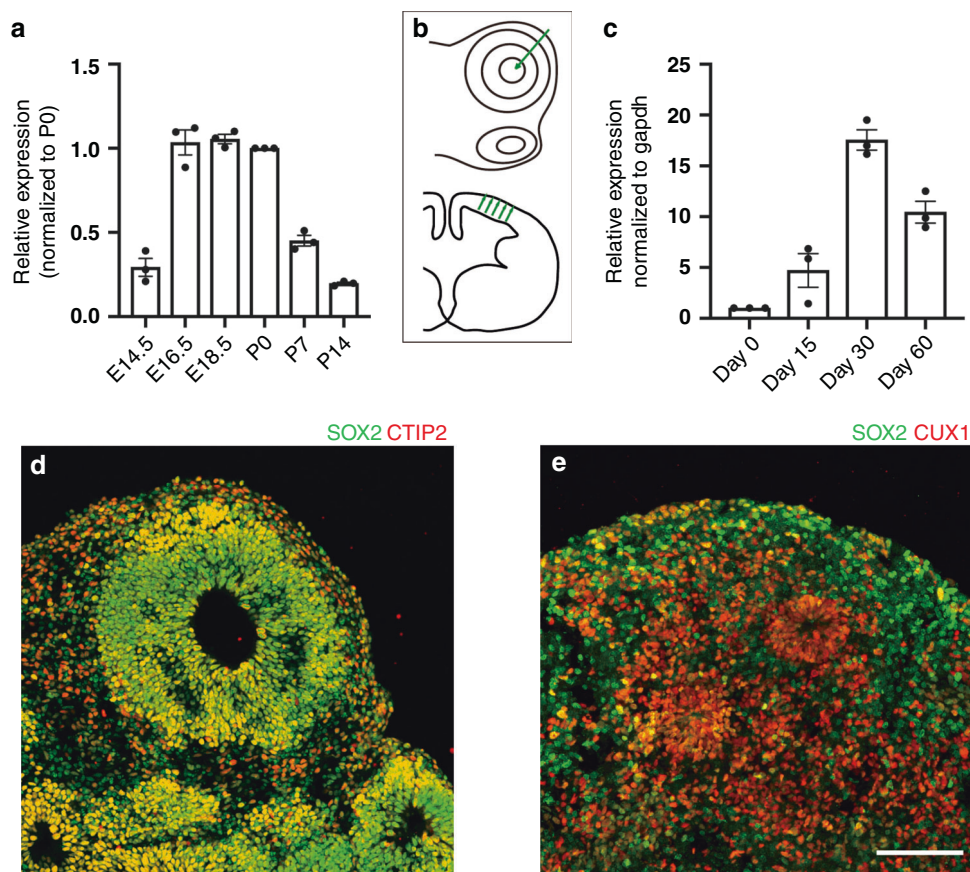


Fig. 1 *Kif5c* is expressed in neurons of the early developing cortex. **a** Quantitative analysis of the *Kif5c* mRNA expression in the mouse early cortical tissues ($n = 3$ pups at each time point) using Q-PCR. The expression level of *Kif5c* in P0 mice was considered as 1. Error bars indicate \pm SEM. **b** Schematic diagram of the development of forebrain organoids that recapitulate the inside-out pattern of human cortical lamination. The pictures indicate the neuronal lamination of the human forebrain organoid (upper panel) and mouse cerebral cortex (lower panel). The green arrows show the direction of neuronal migration. **c** Quantitative analysis of the *Kif5c* mRNA expression level in forebrain organoids ($n = 3$ at each time point) using Q-PCR. The *Kif5c* expression level at DIV0 was considered as 1. Error bars indicate \pm SEM. **d** Example pictures of forebrain organoids stained with SOX2 (green), CTIP2 (red), and CUX1 (red) antibodies. CTIP2 and CUX1 are the marks of the fifth and second layers of the cortical plate, respectively. Scale bar, 100 μ m.

Because genetic diagnostic technology has improved, an increasing number of clinical findings have revealed that KIF gene (*KIF1A*, *KIF2A*, *KIF4A*, *KIF5A*, *KIF5C*, *KIF7*, *KIF11*, and *KIF14*) deficiency is associated with various neurodevelopmental defects^{24–37} (Supplement Table I). With the widespread application of next-generation sequencing technology, several clinical studies have identified mutations in *KIF5C* in patients with MCD, suggesting its critical role in cortical lamination.^{27,28,38–42}

In the present study, we investigated the effects of *Kif5c* knockdown on neurite branching, spine morphology, and cortical migration during early brain development. We found that *Kif5c* is required for proper dendritic branching and spine shaping. *Kif5c* knockdown causes a temporary delay in migration. Furthermore, the expression of a group of genes related to neuronal morphology and migration is altered after *Kif5c* knockdown in cortical neurons. These findings indicate that *Kif5c* is essential for cortical neuron growth and function in the early development stage and provide new insight into the neuronal pathology of *Kif5c*-related MCD in humans.

RESULT

Case series

Eleven cases of *KIF5C* mutation-related MCD have been reported since 2013 (Supplement Table II). According to the summary of clinical and genetic findings, we found that 100% of patients had

malformations of cortical development and microcephaly, 5 patients were diagnosed with pachygyria and 2 with polymicrogyria. Five of six patients with EEG data presented seizures before 1 year of age, 4 patients presented generalized seizures, among which 2 presented intractable seizures. Six of six patients developed severe psychomotor and cognitive impairment and five of five patients presented abnormal behaviors, such as stereotypic hand movements and automutilation. Additionally, nine of eleven patients carried p.E237V hot spot mutations, and the other 2 patients presented p.A268S and p.Y135C mutations. In addition to cortical malformations, some patients also exhibited an abnormal callosum, cerebellum, and increased ventricles. These findings elucidate that *KIF5C* might have a critical role in early human brain development.

Kif5c expression during cerebral cortex maturation

In vertebrates, the *Kif5* gene family has 3 members, *Kif5a*, *5b*, and *5c*. *Kif5b* is widely expressed in all tissues, while *Kif5a* and *Kif5c* are mainly expressed in neurons.²³ We reviewed publicly available single-cell data and found that *KIF5C* was predominantly expressed in the developing cerebral tissue in mice and humans (GSE156793 and GSE132044). We validated the *Kif5c* mRNA levels in the mouse cortical tissue at the early postnatal period using quantitative PCR. We observed increasing *Kif5c* expression after E14.5. The peak expression was detected between E16.5 and P0, and then the expression gradually decreased to a low level (Fig. 1a).

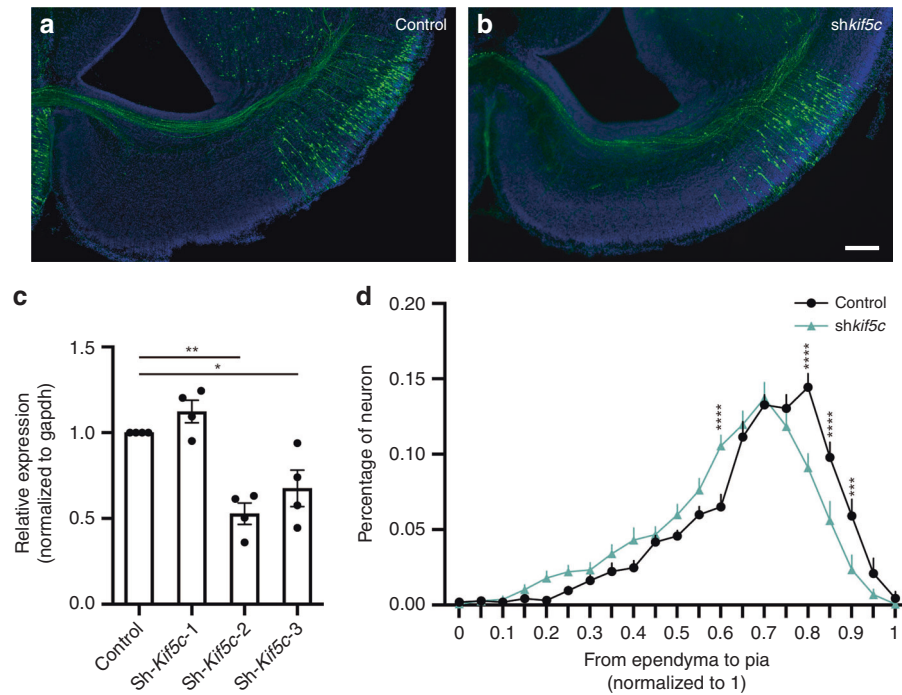


Fig. 2 *Kif5c* knockdown results in delayed neuron migration in vivo. **a, b** Example pictures of E18.5 mouse brain expressed the indicated plasmids using *in utero* electroporation at E13.5. Scale bar, 200 μ m. **c** Quantitation of *Kif5c* mRNA expression levels relative to control (normalized to mouse *Gapdh*). Mouse primary cortical neurons were infected with lentivirus-mediated shRNAs at 0 DIV and harvested at 5 DIV. $**P = 0.0003$ for control vs. sh*Kif5c*-2, $*P = 0.0226$ for control vs. sh*Kif5c*-3, evaluated using Student's *t*-test. Error bars indicate \pm SEM. All data were obtained from three independent experiments. **d** Arrangement of cells expressed indicated shRNAs from the brain ependyma to the pia (a total of 13 pups from 3 dams under each condition were analyzed). Error bars indicate \pm SEM. $****P < 0.0001$ by multiple *t*-tests.

We further examined the *KIF5C* expression pattern during the early development of the human brain. We used human induced pluripotent stem cells (iPSCs) to generate forebrain organoids to investigate *KIF5C* expression. The lamination of forebrain organoids mimics the inside-out pattern of the developing cortex in humans (Fig. 1b).⁴³ *KIF5C* expression was significantly increased and reached the peak level at approximately Day 30, when V layer of the organoid was formed (Fig. 1c). These findings indicate a critical role of *KIF5C* in neuronal lamination. In summary, the expression results of humans and mice suggest that *Kif5c* is pivotal for developing cortical neurons.

***Kif5c* knockdown leads to abnormal cortical neuronal migration**

We performed *in utero* electroporation to reduce *Kif5c* expression in mouse cortical neural progenitors to investigate its role in cortical neuron migration. First, we designed three candidate shRNA (fugw-H1-GFP) targeted *Kif5c* (sh*Kif5c*-#1, sh*Kif5c*-#2, and sh*Kif5c*-#3) and sh*Dsred* as control. Then we infected mouse cortical primary neurons with lentivirus containing those shRNAs. We found that the neurons expressing sh*Kif5c*-#2 showed a significant decrease in the *Kif5c* mRNA level (Fig. 2c). Therefore, sh*Kif5c*-#2 was used in subsequent experiments to reduce *Kif5c* in vivo and in vitro.

We introduced sh*Kif5c*-#2 and sh*Dsred* into the embryonic mouse brain at E13.5, and the embryos were fixed and analyzed at E18.5. These constructs were injected into the lateral brain ventricle. Therefore, the shRNA was only expressed in GFP-labeled cortical ventricular zone (VZ) neurons, allowing us to trace neuronal migration from the VZ. At E18.5, most GFP-expressing neurons left the VZ and arrived at the intermediate zone (IZ) and the cortical plate (CP) in both groups. However, far more sh*Dsred*-expressing neurons reached the surface of the CP than sh*Kif5c*-expressing neurons (Fig. 2).

However, all GFP-labeled neurons of both groups arrived at the surface of the CP at P30, suggesting that early *Kif5c* deficiency leads to a short delay in cortical migration. These results suggest that *Kif5c* is necessary for the precise control of cortical neuron migration.

***Kif5c* knockdown leads to abnormal dendrite branching and spine development in vitro**

Inhibition of kinesin heavy chain expression using antisense oligonucleotides leads to a significant reduction in total neurite length.⁴⁴ Therefore, we knocked down *Kif5c* in primary neurons of the cortex to check whether *Kif5c* is involved in neuronal dendrite growth. Neurons were transfected with sh*Dsred* (control) and sh*Kif5c*-#2 by electroporation at 1 DIV, and then we performed anti-GFP immunostaining at 10 DIV. We found that neurons transfected with sh*Kif5c*-#2 had fewer primary dendrites, but no significant difference in the total dendrite length was found between the sh*Kif5c*-expressing neurons and the controls (Fig. 3). Thus, during early neuronal morphogenesis, *Kif5c* deficiency disturbs dendrite outgrowth in vitro.

After *in utero* electroporation at E13.5, we collected the brain at P30 to analyze the density of dendritic spines with different morphologies. The thin spines in sh*Kif5c*-expressing neurons were denser than those in the control neurons. However, no significant difference in mushroom spines was found between the two groups (Fig. 4). The disturbed spine development might lead to increased neuronal excitability and induce seizures. In the above 6 patients with accessible EEG data, 83% (5/6) had seizures within 1 year of age. Based on these results, *KIF5C* deficiency might contribute to seizures by affecting early dendritic spine development.

In addition, all GFP-labeled cells arrived at the surface of the CP in both the sh*Kif5c* and sh*Dsred* groups, indicating that *kif5c* deficiency

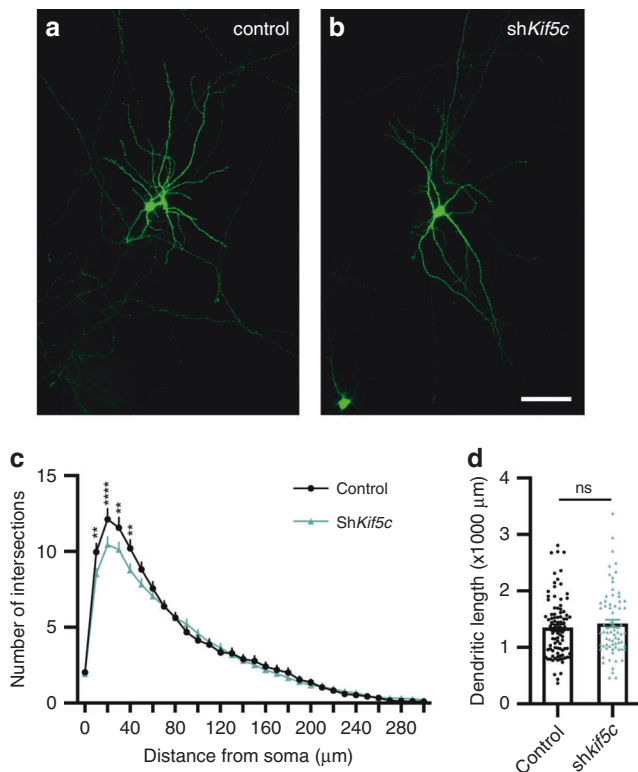


Fig. 3 *Kif5c* regulates dendritic branching in vitro. **a, b** Example pictures of 10 DIV primary neurons transfected with the indicated constructs. Electroporation was performed at 1 DIV and immunolabeling was conducted at 10 DIV. Scale bar, 50 μm . **c** Quantitation of dendritic architecture in neurons collected at 10 DIV using Sholl analysis ($n = 93$ for control and $n = 73$ for *shKif5c*, Fiji, and ImageJ software). $**P(10 \mu\text{m}) = 0.0005$, $***P(20 \mu\text{m}) < 0.0001$, $**P(30 \mu\text{m}) = 0.0005$, $**P(30 \mu\text{m}) = 0.0005$ using multiple *t*-tests. Error bars indicate \pm SEM. **d** Quantitation of the total dendritic length of primary neurons transfected with the indicated plasmids. Error bars indicate \pm SEM. $P = 0.3569$ by Student's *t*-test.

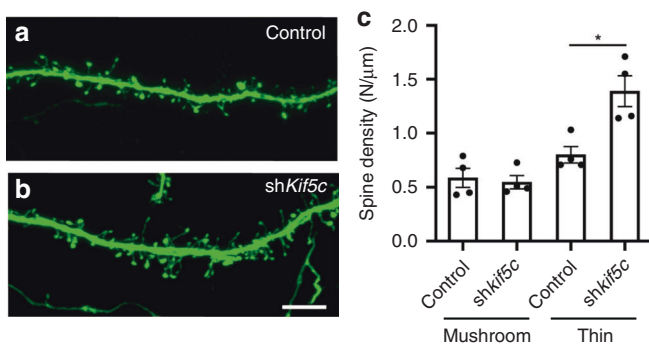


Fig. 4 *Kif5c* knockdown alters the spine morphology. **a, b** Representative images of cortical layers II/III in the mouse brain electroporated with the indicated constructs (apical dendrites, P30, $n = 3$ mice per group). Scale bar, 4 μm . **c** Quantitation of the density of spines with different morphologies (a total of 4 brain slices in each group were randomly analyzed). $*P = 0.0452$ by Student's *t*-test. Error bars indicate SEM.

would not lead to permanent termination of cortical migration. Taken together, *Kif5c* is required for neurite development and thus regulates the establishment of the functional neuronal circuits in the brain.

A neuronal development-associated gene set is differentially expressed between the *shKif5c* and control groups

We collected the total RNA from neurons transfected with lentivirus containing *shKif5c* vs. *shDsred* for RNA sequencing to define the transcriptomic differences between two groups. The mRNA levels of 204 genes were altered in *Kif5c*-deficient neurons compared with control neurons (Fig. 5a). Among these genes, 49 genes were upregulated, and 155 genes were downregulated (adjusted *P*-value < 0.01 , $\log_2(\text{fold-change}) > 1$). Then, a Gene Ontology (GO) analysis of altered genes related to neuronal development was performed (Fig. 5b, c) according to the phenotypes observed in *shKif5c*-expressing neurons in vivo and in vitro. We further validated the alteration of 7 genes, including *Kif5c*, *Itgb1*, *Nrp1*, *Nrp2*, *Gli3*, and *Pafah1b1* (Fig. 5d).

DISCUSSION

Only one *Kif5* gene is expressed in the invertebrates *Drosophila*, *Caenorhabditis elegans*, and *Aplysia*, while 3 *Kif5* variants are expressed in vertebrates, namely, *Kif5a*, *Kif5b*, and *Kif5c*.¹⁰ *Kif5a* and *Kif5c* are mainly expressed in neurons, and *Kif5b* is ubiquitously expressed. The expression of *Kif5c* in the cortex, hippocampus, cerebellum, and spinal cord is 3 to 5 times higher than that of *Kif5a*. These findings indicated that *Kif5c* might play a more important role in the function of the central nervous system (CNS). Although the three *Kif5s* have some functional redundancy,²³ more recent findings have revealed their specific functions. For example, the transport of mitochondria in axons only depends on KIF5A in zebrafish.⁴⁵ Knockdown of *Kif5b* and *Kif5c* leads to a significant reduction in the number of dendritic spines on mouse primary cortical neurons, while *Kif5a* deficiency does not affect spine development.⁴⁶ Clinical findings showed that *KIF5A* deficits cause spastic paraplegia 10 (SPG 10, OMIM#602821) and neonatal intractable myoclonus (NEIMY, OMIM# 617235). Recently, several cases carrying rare *KIF5C* mutations have been reported. All of these patients presented microcephaly and malformation of cortical development (such as polymicrogyria, pachygyria, and cortical dysplasia), and some had experienced seizures beginning at an early age, suggesting its deficiency might lead to early neuronal development abnormalities.

We found that *Kif5c* is expressed at high levels during early brain development and *Kif5c* deficiency leads to abnormal neuronal morphology and radial migration. By performing an embryonic electroporation study, we found that *Kif5c* deficiency leads to an increased density of thin spines on cortical neurons during early brain development in vivo. Swarnkar et al. also reported a significant increase in the number of thin spines following *Kif5c* knockdown, but the number of mushroom spines was reduced.⁴⁷ However, Zhao et al. observed reductions in the densities of both thin and mushroom spines following *Kif5c* knockdown in hippocampal neurons in vitro.⁴⁶ Willemsen et al. found that *KIF5C*-E237K, the hot spot mutation, showed a significant reduction in distal neurite localization, which led to a significant decrease in the mEPSC amplitude.²⁸ Based on these findings, *Kif5c* deficiency might cause disease by contributing to abnormal synaptic function. However, unlike the human brain, the mouse brain has no gyrus. Therefore, in addition to a smaller brain size of the mice with *kif5c* gene knockout, the nervous system does not show apparent malformations.²³

A traditional claim is that proteins are synthesized in the neuronal soma and then conveyed to the terminals in membranous organelles or protein complexes. However, a group of mRNAs is delivered to neurite terminals to carry out local protein synthesis.⁴⁸ *KIF5C*, which is involved in transporting cargos (including vesicles, membranous organelles, protein complexes,

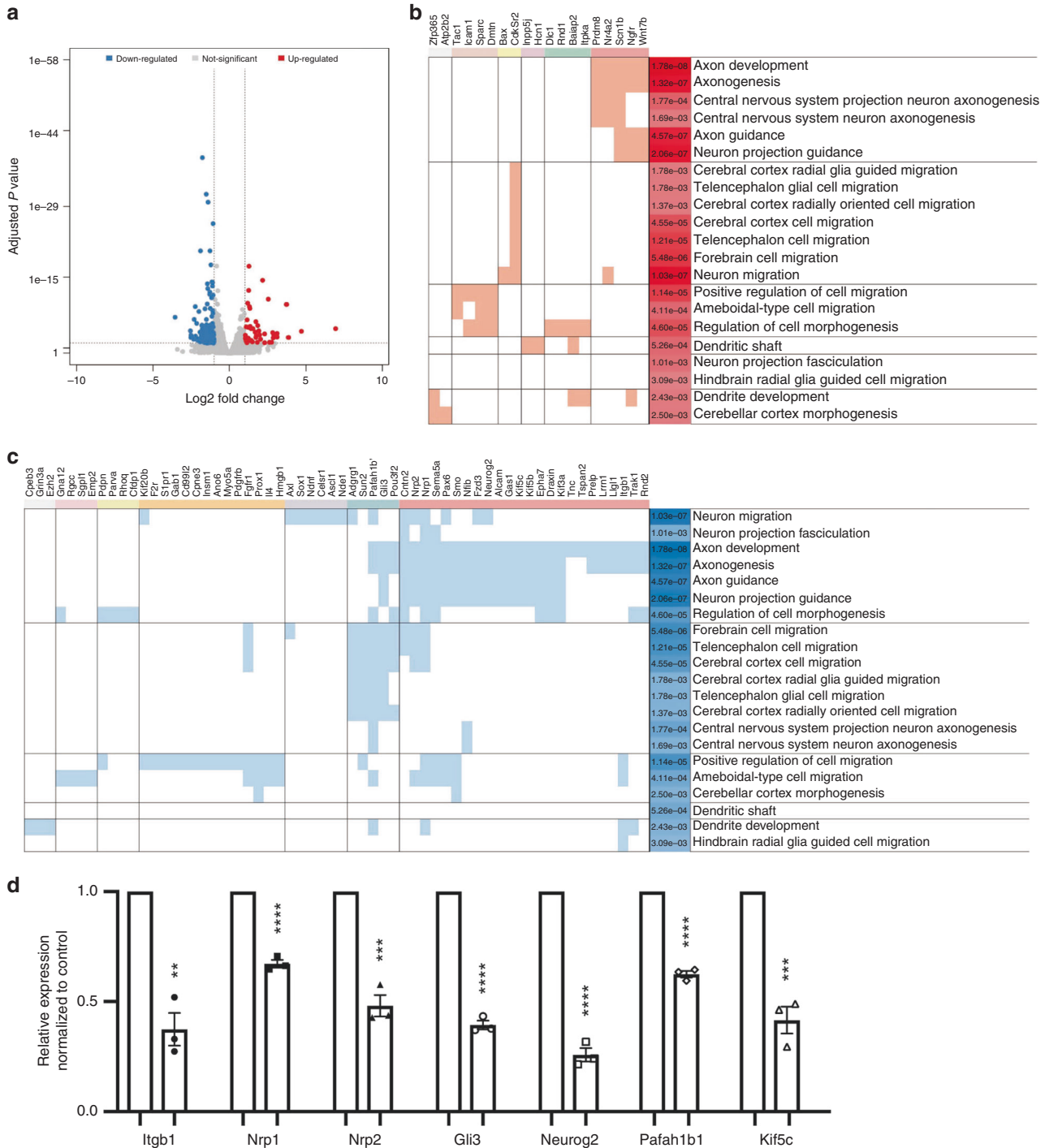


Fig. 5 GO analysis of differentially expressed genes in neurons after *Kif5c* knockdown. **a** Differentially expressed transcripts (highlighted in color, adjusted *P*-value < 0.01, log₂(fold-change) > 1) between cortical neurons transfected with lentiviruses containing *shKif5c* and *shDred* (control). **b, c** Gene Ontology (GO) analysis of altered genes related to neuronal development in cortical neurons after *Kif5c* knockdown compared with the control (**b** for upregulated and **c** for downregulated). Each subfigure shows a heat map clustered on rows and columns separately to visualize the genes enriched in each GO term. Colored boxes in the matrix represent differentially expressed genes (columns) belonging to GO terms (rows). Genes and GO terms were clustered in the existing binary matrix, and genes or GO terms with similar expression patterns were grouped (different groups were separated by black lines). Adjusted *P*-values (BH) for enriched GO terms are shown at the left of the corresponding term, with darker colors indicating greater significance. **d** Validation of altered genes using real-time PCR analysis. Data are presented as the means ± SEM; *n* = 3 experiments; ***P*(*Itgb1*) = 0.0011, *****P*(*Nrp1*) < 0.0001, ****P*(*Nrp2*) = 0.0004, *****P*(*Gli3*) < 0.0001, *****P*(*Neurog2*) < 0.0001, *****P*(*Pafah1b1*) < 0.0001, ****P*(*Kif5c*) = 0.0007.

mRNAs, and chromosomes) from the minus end of microtubules to the plus end in neurites, is implicated in regulating local mRNA transport.⁴⁹ In the present study, we harvested cortical neurons transfected with control or *shkif5c* plasmid. Then we found that

Kif5c knockdown affects the mRNA levels of pivotal genes—*Itgb1*, *Nrp1*, *Nrp2*, *Gli3*, *Neurog2*, and *Pafah1b1*—related to neurite development and neuronal migration (Fig. 5d).

The cell surface receptors *Itgb1*, *Nrp1*, and *Nrp2* have critical roles in regulating cortical neuronal migration during early brain development, and *Nrp1* is also involved in neocortical dendrite development.^{50–55} Conditional knockout of *Gli3* causes neuronal overmigration, resulting in an enlarged brain and abnormally folded structures.⁵⁶ *Neurog2* deficiency leads to cortical migration defects and changes in dendrite morphology.^{57,58} *Pafah1b1* knockout studies revealed its essential function in the regulation of neuronal migration, progenitor cell proliferation, and synaptic E/I balance in the dentate gyrus.^{59–63} However, the mechanism by which *kif5c* deficiency alters the mRNA levels of these genes and whether it affects their local protein synthesis by modifying neurite transportation require further study.

METHODS

Plasmids

The sh*Kif5c* (#1, #2, #3, and *Dsred*) was generated by inserting the annealed oligonucleotide primers into the FUGW-H1 construct (Addgene, 14883) using *XbaI*–*Bam*HI cloning sites. Primers' sequences are listed in Supplement Table III.

RNA extraction and reverse transcription

After anesthetized with pentobarbital sodium and sacrificed, we isolated the cortical area of the brain in pre-cooled PBS according to the map of The Mouse Brain in Stereotaxic Coordinates.⁶⁴ We isolated total RNA from the cortical brain under manufacturer's instructions of TRIzol™ Reagent (Invitrogen, 15596018) and then reversed the RNA by the Reverse Transcriptase M-MLV kit (TaKaRa, D2639B).

Quantitative real-time PCR

The mRNA expression level of indicated genes was measured through quantitative real-time PCR (Q-PCR) using SYBR green (Toyobo, QPK-201). The internal control is mouse *Gapdh* or *Rpl191* or human *GAPDH* gene. The primer sequences are listed in Supplement Table III.

The culture and transfection of primary cortical neurons

Cortical tissues of E13.5 mouse embryos were minced and digested with 20 U/ml papain (Worthington, LS003126) to obtain dissociated neurons.⁶⁵ Two neuronal transfection methods were used in our study. For assessing KD efficiency and transcriptomic experiments, we packaged the shRNAs into lentivirus for higher transfection efficiency. For the dendrite branching experiment, neurons and plasmids were mixed and resuspended in the Nucleofector Solution buffer and then electrotransfected using the "mouse, neuron, 0–005" process on the AMAXA nucleofector II device (AAD-1001S, Germany), in which the neuron viability was over 80%. In Lab-Tek II chamber slides (ThermoFisher Scientific, 154941), Cells were fed with Neurobasal medium (Gibco, 21103-049) supplemented with 2 mM Glutamax-I (Gibco, 35050-061) and 0.2% B27 (Gibco, 17504-044). We mixed the transfected neurons with untreated neurons in a ratio of 1:8 for sparse labeling.

In utero electroporation

In utero electroporation was performed using the previously reported methods.⁶⁶ Firstly, E13.5 pregnant mice (C57BL/6J, RRID: IMSR_JAX: 000664) were intraperitoneally injected with 0.7% pentobarbital sodium (10 µl/g per mouse) to achieve deep anesthesia. Plasmids (sh*Dsred* or sh*Kif5c*, 2 µg/µl) with Fast Green (0.05%, Sigma) were injected into the ventricle using a glass micropipette by an experimenter who was blinded to the groups. In each embryo, only one side of the brain ventricle was injected with constructs. Plasmids were then delivered into the ventricular zone (VZ) cells by applying 5 electric pulses at 30 V for 50 ms at 1 s intervals using the Electro Square Porator (ECM 830, BTX, San Diego, CA). After closing the abdomen, mice were left to recover from anesthesia on a warm blanket. Pup's brains were harvested at E18.5 or P30, then were fixed with 4% PFA and dehydrated in sucrose solutions.

Generation of forebrain organoids derived from human iPSCs

Forebrain organoids were produced following the previously published methods.⁶⁷ For the first 4 days, human iPSCs were cultured with neural induction medium (NIM), which consists of DMEM/F12, 1xGlutaMAX, 1xN2, 1xNEAA, 2 µM dorsomorphin (Sigma-Aldrich), and 2 µM SB-431542 (Tocris).

On days 5–6, the culture medium was half changed with differentiation medium (DM), which includes DMEM/F12, 1xGlutaMAX, 1xN2, 1xNEAA, 1 µM CHIR (Cellgientech), and 2 µM SB-431542. Then the organoids were embedded in Matrigel (BD Biosciences) and cultivated in cortical DM for another 7 days. On day 14, embedded organoids were gently separated from the Matrigel and cultured in DM supplemented with 1x B27 (Invitrogen), 1x 2-mercaptoethanol, and 2.5 µg/ml insulin (Sigma). The forebrain organoids were harvested on Days 15, 30, and 60 for subsequent experiments.

Immunohistochemical staining and image analysis

All the sample sections on slices were produced using the Leica freezing microtome (CM1950). The neurons, brain slices, and forebrain organoid slices were all fixed with 4% PFA and blocked at room temperature. The composition of the blocking buffer is slightly different. For cultured neurons, the blocking buffer is 3% BSA and 0.1% Triton X-100 in PBS. For brain and organoid slices, the buffer is 5% BSA and 0.3% Triton X-100 in PBS. Then the slices were incubated with indicated antibodies in a blocking buffer of 3% BSA and 0.1% Triton X-100. The following antibodies were used: anti-GFP (rabbit, Invitrogen, A11122): 1:1000, anti-CTIP2 (rat, Abcam, #ab18465): 1:300, anti-SOX2 (goat, R&D, AF2018): 1:500, and anti-CUX1 (mouse, Santa Cruz, sc_514008): 1:500. For immunohistochemical staining, organoid slices were stained with 2 cortical layer markers (CTIP2: Layer V and CUX1: Layer II) to examine developmental milestones.

All images were analyzed using ImageJ software (RRID: SCR_003070). For the dendrite branching experiments, the center of the cell soma was taken as the starting point when calculating the length of a primary dendrite. Slices labeling was blinded to the person who recorded the images to prevent selection bias.

Transcriptome sequencing and analysis

Sequencing libraries were generated using NEBNext® Ultra™ RNA Library Prep Kit for Illumina™ following the manufacturer's recommendations. The clean data were obtained by removing reads containing adapter, ploy-N, and low-quality reads from raw data. Index of the reference genome was built and paired-end clean reads were aligned to the reference genome using Hisat2 v2.0.5. FeatureCounts v1.5.0-p3 was used to count the reads numbers mapped to each gene. And then Reads/Fragments Per Kilobase Million Reads (FPKM) of each gene was calculated based on the length of the gene and reads count mapped to this gene. Differential expression analysis of two groups was performed using the DESeq2 R package (1.16.1). Gene Ontology (GO) enrichment analysis of differentially expressed genes was implemented by the clusterProfiler R package. Significant differentially expressed genes were determined as those with adjusted *P*-values < 1e−4 and log2(fold-change) (FC) > 0.4.

Statistics

Comparisons between two groups were performed using a Two-tailed Student's *t*-test, and multiple *t*-tests were used for the curves (dendrite branching and neuronal migration). GraphPad Prism 8 (www.graphpad.com) software was used for statistical analysis. Data are shown as the means ± SEM, and *P*-values are reported in the figure legend (statistical significance was determined at *P* < 0.05). The in vitro experiments were performed at least 3 times independently and at least 3 mice from 2 different litters were used. For migration experiments, we used one E13.5 mouse each time to minimize the bias caused by individual differences and repeated the operation three times independently. At E18.5, we collected all embryonic brains from three independent experiments, and the brains were selected under a fluorescence dissecting microscope (Nikon 80i, MBA75020, Japan). Only those with EGFP expression were retained for further immunofluorescence staining (Supplement Fig. I).

Study approval

All animal experiments were performed according to the Biomedical Research Ethics Committee guidelines of the Shanghai Institutes for Biological Science.

REFERENCES

- Rakic, P. Specification of cerebral cortical areas. *Science* **241**, 170–176 (1988).
- Barkovich, A. J., Guerrini, R., Kuzniecky, R. I., Jackson, G. D. & Dobyns, W. B. A developmental and genetic classification for malformations of cortical development: update 2012. *Brain* **135**, 1348–1369 (2012).

3. Francis, F. et al. Human disorders of cortical development: from past to present. *Eur. J. Neurosci.* **23**, 877–893 (2006).
4. Guerrini, R., Dobyns, W. B. & Barkovich, A. J. Abnormal development of the human cerebral cortex: genetics, functional consequences and treatment options. *Trends Neurosci.* **31**, 154–162 (2008).
5. Ostergaard, P. et al. Mutations in Kif11 cause autosomal-dominant microcephaly variably associated with congenital lymphedema and chorioretinopathy. *Am. J. Hum. Genet.* **90**, 356–362 (2012).
6. Mulvey, B. & Dougherty, J. D. Weaving new insights for the genetic regulation of human cognitive phenotypes. *Cell* **172**, 10–13 (2018).
7. Arikath, J. Molecular mechanisms of dendrite morphogenesis. *Front. Cell Neurosci.* **6**, 61 (2012).
8. Granato, A. & De Giorgio, A. Alterations of neocortical pyramidal neurons: turning points in the genesis of mental retardation. *Front. Pediatr.* **2**, 86 (2014).
9. Mischel, P. S., Nguyen, L. P. & Vinters, H. V. Cerebral cortical dysplasia associated with pediatric epilepsy - review of neuropathologic features and proposal for a grading system. *J. Neuropathol. Exp. Neurol.* **54**, 137–153 (1995).
10. Miki, H., Setou, M., Kaneshiro, K. & Hirokawa, N. All kinesin superfamily protein, Kif, genes in mouse and human. *Proc. Natl Acad. Sci. USA* **98**, 7004–7011 (2001).
11. Mandelkow, E. & Mandelkow, E. M. Kinesin motors and disease. *Trends Cell Biol.* **12**, 585–591 (2002).
12. Lawrence, C. J. et al. A standardized kinesin nomenclature. *J. Cell Biol.* **167**, 19–22 (2004).
13. Hirokawa, N., Niwa, S. & Tanaka, Y. Molecular motors in neurons: transport mechanisms and roles in brain function, development, and disease. *Neuron* **68**, 610–638 (2010).
14. Homma, N. et al. Kinesin superfamily protein 2a (Kif2a) functions in suppression of collateral branch extension. *Cell Struct. Funct.* **29**, 55–55 (2004).
15. Yonekawa, Y. et al. Defect in synaptic vesicle precursor transport and neuronal cell death in Kif1a motor protein-deficient mice. *J. Cell Biol.* **141**, 431–441 (1998).
16. Marszalek, J. R., Ruiz-Lozano, P., Roberts, E., Chien, K. R. & Goldstein, L. S. B. Situs inversus and embryonic ciliary morphogenesis defects in mouse mutants lacking the Kif3a subunit of kinesin-II. *Proc. Natl Acad. Sci. USA* **96**, 5043–5048 (1999).
17. Nonaka, S. et al. Randomization of left-right asymmetry due to loss of nodal cilia generating leftward flow of extraembryonic fluid in mice lacking Kif3b motor protein (Vol 95, Pg 829, 95). *Cell* **99**, 117 (1999).
18. Zhao, C. et al. Charcot-Marie-Tooth disease type 2a caused by mutation in a microtubule motor Kif1bbeta. *Cell* **105**, 587–597 (2001).
19. Midorikawa, R., Takei, Y. & Hirokawa, N. Kif4 motor regulates activity-dependent neuronal survival by suppressing Parp-1 enzymatic activity. *Cell* **125**, 371–383 (2006).
20. Tanaka, Y. et al. Targeted disruption of mouse conventional kinesin heavy chain, Kif5b, results in abnormal perinuclear clustering of mitochondria. *Cell* **93**, 1147–1158 (1998).
21. Xia, C. H. et al. Abnormal neurofilament transport caused by targeted disruption of neuronal kinesin heavy chain Kif5a. *J. Cell Biol.* **161**, 55–66 (2003).
22. Encalada, S. E., Szpankowski, L., Xia, C. H. & Goldstein, L. S. B. Stable kinesin and dynein assemblies drive the axonal transport of mammalian prion protein vesicles. *Cell* **144**, 551–565 (2011).
23. Kanai, Y. et al. Kif5c, a novel neuronal kinesin enriched in motor neurons. *J. Neurosci.* **20**, 6374–6384 (2000).
24. Nemami, T. et al. Kif1a-related disorders in children: a wide spectrum of central and peripheral nervous system involvement. *J. Peripheral Nerv. Syst.* **25**, 117–124 (2020).
25. Riviere, J. B. et al. Kif1a, an axonal transporter of synaptic vesicles, is mutated in hereditary sensory and autonomic neuropathy type 2. *Am. J. Hum. Genet.* **89**, 219–230 (2011).
26. Pennings, M. et al. Kif1a variants are a frequent cause of autosomal dominant hereditary spastic paraplegia. *Eur. J. Hum. Genet.* **28**, 40–49 (2020).
27. Poirier, K. et al. Mutations in Tubg1, Dync1h1, Kif5c and Kif2a cause malformations of cortical development and microcephaly. *Nat. Genet.* **45**, 639 (2013).
28. Willemsen, M. H. et al. Involvement of the kinesin family members Kif4a and Kif5c in intellectual disability and synaptic function. *J. Med. Genet.* **51**, 487–494 (2014).
29. Nicolas, A. et al. Genome-wide analyses identify Kif5a as a novel Als gene. *Neuron* **97**, 1268 (2018).
30. Rydzanicz, M. et al. Kif5a de novo mutation associated with myoclonic seizures and neonatal onset progressive leukoencephalopathy. *Clin. Genet.* **91**, 769–773 (2017).
31. Crimella, C. et al. Mutations in the motor and stalk domains of Kif5a in spastic paraplegia type 10 and in axonal Charcot-Marie-Tooth type 2. *Clin. Genet.* **82**, 157–164 (2012).
32. Ali, B. R., Silhavy, J. L., Akawi, N. A., Gleeson, J. G. & Al-Gazali, L. A. Mutation in Kif7 is responsible for the autosomal recessive syndrome of macrocephaly, multiple epiphyseal dysplasia and distinctive facial appearance. *Orphanet. J. Rare Dis.* **7**, 27 (2012).
33. Putoux, A. et al. Kif7 mutations cause fetal hydrolethals and acrocallosal syndromes. *Nat. Genet.* **43**, U601–U147 (2011).
34. Dafinger, C. et al. Mutations in Kif7 link Joubert syndrome with sonic hedgehog signaling and microtubule dynamics. *J. Clin. Investig.* **121**, 2662–2667 (2011).
35. Birtel, J. et al. Novel insights into the phenotypical spectrum of Kif11-associated retinopathy, including a new form of retinal ciliopathy. *Invest. Ophthalm. Vis. Sci.* **58**, 3950–3959 (2017).
36. Filges, I. et al. Exome sequencing identifies mutations in Kif14 as a novel cause of an autosomal recessive lethal fetal ciliopathy phenotype. *Clin. Genet.* **86**, 220–228 (2014).
37. Makrythanasis, P. et al. Biallelic variants in Kif14 cause intellectual disability with microcephaly. *Eur. J. Hum. Genet.* **26**, 330–339 (2018).
38. Cavallin, M. et al. Recurrent Kif5c mutation leading to frontal pachygyria without microcephaly. *Neurogenetics* **17**, 79–82 (2016).
39. Al-Shamsi, A., Hertecant, J. L., Souid, A. K. & Al-Jasmi, F. A. Whole exome sequencing diagnosis of inborn errors of metabolism and other disorders in United Arab Emirates. *Orphanet. J. Rare Dis.* **11**, 94 (2016).
40. Michels, S. et al. Mutations of Kif5c cause a neurodevelopmental disorder of infantile-onset epilepsy, absent language, and distinctive malformations of cortical development. *Am. J. Med. Genet. A* **173**, 3127–3131 (2017).
41. Duquesne, S., Nassogne, M. C., Clapuyt, P., Stouffs, K. & Sznajer, Y. Phenotype description in Kif5c gene hot-spot mutations responsible for malformations of cortical development (Mcd). *Eur. J. Med. Genet.* **63**, 103991 (2020).
42. Jamuar, S. S. & Walsh, C. A. Somatic mutations in cerebral cortical malformations. *N. Engl. J. Med.* **371**, 2038–2038 (2014).
43. Kriegstein, A. R. & Noctor, S. C. Patterns of neuronal migration in the embryonic cortex. *Trends Neurosci.* **27**, 392–399 (2004).
44. Ferreira, A., Niclas, J., Vale, R. D., Banker, G. & Kosik, K. S. Suppression of kinesin expression in cultured hippocampal-neurons using antisense oligonucleotides. *J. Cell Biol.* **117**, 595–606 (1992).
45. Campbell, P. D. et al. Unique function of kinesin Kif5a in localization of mitochondria in axons. *J. Neurosci.* **34**, 14717–14732 (2014).
46. Zhao, J. J. et al. Specific depletion of the motor protein Kif5b leads to deficits in dendritic transport, synaptic plasticity and memory. *Elife* **9**, e53456 (2020).
47. Swamkar, S. et al. Molecular motor protein Kif5c mediates structural plasticity and long-term memory by constraining local translation. *Cell Rep.* **36**, 109369 (2021).
48. Hirokawa, N. & Takemura, R. Molecular motors and mechanisms of directional transport in neurons. *Nat. Rev. Neurosci.* **6**, 201–214 (2005).
49. Kanai, Y., Dohmae, N. & Hirokawa, N. Kinesin transports rna: isolation and characterization of an RNA-transporting granule. *Mol. Biol. Cell* **15**, 118a (2004).
50. Graus-Porta, D. et al. Beta1-class integrins regulate the development of laminae and folia in the cerebral and cerebellar cortex. *Neuron* **31**, 367–379 (2001).
51. Huang, Z. et al. Distinct roles of the beta 1-class integrins at the developing and the mature hippocampal excitatory synapse. *J. Neurosci.* **26**, 11208–11219 (2006).
52. Liu, W. et al. Marveld1 depletion leads to dysfunction of motor and cognition via regulating glia-dependent neuronal migration during brain development. *Cell Death Dis.* **9**, 999 (2018).
53. Andrews, W. D., Barber, M., Nemitz, M., Memi, F. & Parnavelas, J. G. Semaphorin3a-Neuropilin1 signalling is involved in the generation of cortical interneurons. *Brain Struct. Funct.* **222**, 2217–2233 (2017).
54. Kanatani, S. et al. The Coup-Tfi/Neuropilin-2 is a molecular switch steering diencephalon-derived gabaergic neurons in the developing mouse brain. *Proc. Natl Acad. Sci. USA* **112**, E4985–E4994 (2015).
55. Kohno, T. et al. Reelin-Nrp1 interaction regulates neocortical dendrite development in a context-specific manner. *J. Neurosci.* **40**, 8248–8261 (2020).
56. Zhang, L. et al. Counter-balance between Gli3 and Mir-7 is required for proper morphogenesis and size control of the mouse brain. *Front. Cell Neurosci.* **12**, 259 (2018).
57. Avansini, S. H. et al. Dysregulation of Neurog2 plays a key role in focal cortical dysplasia. *Ann. Neurol.* **83**, 623–635 (2018).
58. Hand, R. et al. Phosphorylation of Neurogenin2 specifies the migration properties and the dendritic morphology of pyramidal. *Neurons Neocortex. Neuron* **48**, 45–62 (2005).
59. Dinday, M. T., Girsakis, K. M., Lee, S., Baraban, S. C. & Hunt, R. F. Pafah1b1 haploinsufficiency disrupts Gaba neurons and synaptic E/I balance in the dentate gyrus. *Sci. Rep.* **7**, 8269 (2017).
60. Hirotsune, S. et al. Graded reduction of Pafah1b1 (Lis1) activity results in neuronal migration defects and early embryonic lethality. *Nat. Genet.* **19**, 333–339 (1998).
61. Katayama, K. I., Hayashi, K., Inoue, S., Sakaguchi, K. & Nakajima, K. Enhanced expression of Pafah1b1 causes over-migration of cerebellar cortical neurons into the marginal zone. *Brain Struct. Funct.* **222**, 4283–4291 (2017).
62. Pramparo, T., Youn, Y. H., Yingling, J., Hirotsune, S. & Wynshaw-Boris, A. Novel embryonic neuronal migration and proliferation defects in DCX mutant mice are exacerbated by Lis1 reduction. *J. Neurosci.* **30**, 3002–3012 (2010).

63. Wynshaw-Boris, A. Lissencephaly and Lis1: insights into the molecular mechanisms of neuronal migration and development. *Clin. Genet.* **72**, 296–304 (2007).
64. Paxinos, G. & Franklin, K. B. J. *The Mouse Brain in Stereotaxic Coordinates* 2nd edn (Academic Press, 2001).
65. Yu, X. & Malenka, R. C. Beta-catenin is critical for dendritic morphogenesis. *Nat. Neurosci.* **6**, 1169–1177 (2003).
66. Saito, T. In vivo electroporation in the embryonic mouse central nervous system. *Nat. Protoc.* **1**, 1552–1558 (2006).
67. Qian, X. Y. et al. Brain-region-specific organoids using mini-bioreactors for modeling Zikv exposure. *Cell* **165**, 1238–1254 (2016).

AUTHOR CONTRIBUTIONS

W.L. and W.Z. carried out substantial contributions to conception and design. W.L. and T.C. performed the experiments. W.L., X.D., H.C., and L.Y. conducted analysis and interpretation of data. W.L. drafted and revised the article. W.Z. and Z.Q. provided critical revision of the manuscript and approved the final version for publication. This work obtained funding from Z.Q. and W.Z.

FUNDING

This work was funded by the Shanghai Municipal Science and Technology Major Project (Grant Nos. 2017SHZDZX01, 2018SHZDZX05, 20Z11900600).

COMPETING INTERESTS

The authors declare no competing interests.

ADDITIONAL INFORMATION

Supplementary information The online version contains supplementary material available at <https://doi.org/10.1038/s41390-021-01922-8>.

Correspondence and requests for materials should be addressed to Wenhao Zhou.

Reprints and permission information is available at <http://www.nature.com/reprints>

Publisher's note Springer Nature remains neutral with regard to jurisdictional claims in published maps and institutional affiliations.